SOILS AND FOUNDATIONS Vol. 50, No. 5, 609–621, Oct. 2010
Japanese Geotechnical Society

BEHAVIOR OF LARGE SCALE UNDERGROUND CAVERN LOCATED IN JOINTED ROCK MASSES EVALUATED BY USING DISTINCT ELEMENT METHOD

Bo Li[i], Yujing Jiang[ii),iii)], Yoshihiko Tanabashi[ii)] and Yuji Yamashita[iv)]

ABSTRACT

The stability and support effects of large-scale underground caverns located in jointed rock masses are principally ruled by the mechanical behavior of discontinuities. The major deformations of the host rock masses containing underground caverns originate from the normal and shear movements among the walls of discontinuities. Therefore, in the numerical simulations of the deformation behavior of underground structures, how to accurately model the discontinuities becomes a key problem. In this study, a 2-D distinct element code, UDEC, was used to analyze the deformation behavior of an underground cavern of a pumped storage power plant, based on in-situ geological data. The validity of numerical simulation was evaluated by comparing the numerical results with the site measurement data at two cross-sections of the cavern. Some local deformation behavior of the cavern affected by the characteristics of discontinuity distributions was discussed. The influences of cross-sectional shape of the cavern and the orientation of initial ground stress on the performance of cavern were evaluated. The simulation results revealed that the orientation, position and density of discontinuities as well as the cross-sectional shape of a carven influence its deformation behavior and stability significantly.

Key words: deformation, discontinuity, distinct element method, excavation, measurement, underground cavern (**IGC**: G2/G5/H5)

INTRODUCTION

In recent years, underground space has been increasingly developed due to the issues like limitation of urban ground, environmental protection, and economical consideration. To effectively implement the design, construction and management of an underground structure, the deformation behavior of the rock masses encompassing the structure need to be adequately evaluated. The discontinuities existing in rock masses have various lengths, orientations, spacing and gaps, exhibiting anisotropic characteristics, which could significantly affect the stability of an underground structure. To effectively assess the stability of an underground structure, the adequate representations of the mechanical behavior and distribution properties of discontinuities in numerical models are required.

Various numerical approaches based on different theories have been adopted to analyze the behavior of underground structures in discontinuous rock masses, in most of which, the discontinuities have been specially treated to facilitate modelling. In the finite element method (FEM), the jointed rock mass is often modelled as an equivalent continuum. Some special treatments, such as simplifying the joints as slidelines (Schwer and Lindberg, 1992) in the finite difference method (FDM), have been adopted to improve the representation of discontinuities in the continuum-based analyses. These treatments, however, can only be applied when the number of discontinuities and their displacements are small (Zhao and Chen, 1998). In the discrete element method (DEM), the rock mass is represented as an assemblage of discrete blocks and the discontinuities as interfaces between blocks, which facilitate the modelling of the mechanical behavior (compression, slip, separation etc.) and geometrical properties (orientation, gap, spacing etc.) of discontinuities according to site investigation data and therefore is considered as a better approach to study the problems in discontinuous rock masses. A number of parametric studies have been carried out using DEM to estimate the behavior of rock masses with or without cavern, with one set or more than one set of discontinuities (Kulatilake et al., 1992; Cundall, 1993; Souley and Homand, 1996; Shne and Barton, 1997; Bhasin and

i) Assistant Professor, Faculty of Engineering, Nagasaki University, Japan (libo@stu.civil.nagasaki-u.ac.jp).
ii) ditto.
iii) Research Center for Geo-Environmental Science, Dalian University, P.R. China.
iv) Kyushu Electric Power Co., Inc., Japan.
The manuscript for this paper was received for review on July 22, 2008; approved on May 19, 2010.
Written discussions on this paper should be submitted before May 1, 2011 to the Japanese Geotechnical Society, 4-38-2, Sengoku, Bunkyo-ku, Tokyo 112-0011, Japan. Upon request the closing date may be extended one month.

Hoeg, 1998; Zhao and Chen, 1998; Suorineni et al., 1999; Hao and Azzam, 2005; Jiang et al., 2006). The DEM has also been applied to the construction sites containing underground structures and the numerical results have been compared with the measured performance (Bhasin et al., 1996; Souley et al., 1997). However, the cases using DEM to assess the performance of underground caverns are still few, and the standard routine of DEM modelling, such as the determination of mechanical properties and the modelling procedure have not been established.

Nowadays, the behavior evaluations of large-scale underground caverns are usually conducted by using 3-D simulations. In some circumstances (e.g., the cross-sectional shape of cavern is regular, the in-situ stresses are vertical or parallel to the cavern axis), the 2-D simulations (e.g., 2-D DEM) could also be a useful tool to help understand the performance of typical cross-section of cavern, especially to assess the local deformation behavior in the cross-sections with unfavorable ground conditions like joints encountering the cavern wall. The reliability of the simulation results by using 2-D DEM depends on the accuracy of input mechanical properties and geometrical distribution of discontinuities. In this study, the excavation process of the cavern of a pumped storage power plant was reproduced and the discontinuities distributed in the host rock masses were modelled according to the geological data by using the distinct element code UDEC (Itasca Consulting Group, Inc., 1998). The deformation behavior along a series of measuring lines at various positions of the cavern has been analyzed and the mechanism of several local deformations influenced by the presence of rock joints was clarified. Necessary geological survey for assessing the stability of a cavern in required accuracy was proposed, and the process starting from deciding mechanical properties for numerical simulation, to the disposal of simulation results has been clearly presented. The influences of cross-sectional shape and orientation of initial ground stress on the mechanical behavior of the underground cavern were estimated through parametric studies based on one cross-sectional profile of the opening. The numerical predictions along with the step-by-step excavation process agree well with the field measurements.

FIELD LAYOUT AND NUMERICAL MODEL

The modelling objective of this study is the powerhouse of Omaru pumped storage power plant located in Miyazaki prefecture, Japan. This underground powerhouse is 425 m in depth from the ground surface (the apex of a mountain) with a warhead shaped cross-sectional profile as shown in Fig. 1. The height, width and length of the powerhouse are 48 m, 24 m and 187 m, respectively. The excavated volume of the rock mass is around 160,000 m^3 and the maximum cross-sectional area is about 1,000 m^2. Four power generators, each one having a generating capacity of 300,000 KW (totally 1.2 million KW) and two transformers are installed in the

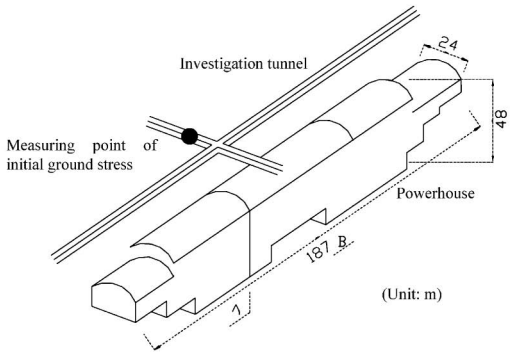

(a) Sketch view of the powerhouse. The cross-sections A and B are chosen to generate numerical models

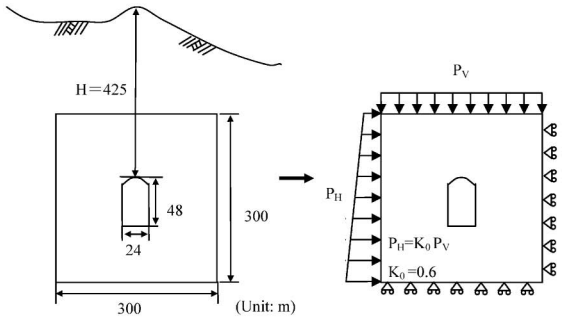

(b) Location of the study area and boundary conditions of the numerical model. Where P_H and P_V are vertical and horizontal pressures respectively, K_0 is the coefficient of lateral pressure

Fig. 1. Illustration of the location and dimension of the objective cavern in this study and the boundary conditions of the numerical model taking into account the initial ground stresses

powerhouse. The cavern is located in slightly weathered granodiorite, the main part of which was classified as class C_H with a few discrete parts classified as C_M according to the rock mass classification standard of Japan (JSMS, 2002). The unconfined compression strength of the C_H type intact rock is 170 MPa. The strike of the cavern axis is N10°E. The measured initial ground stresses are as follows: 1) $\sigma_1 = 6.0 \pm 2.1$ MPa, strikes N96°E and dips 77°; 2) $\sigma_2 = 4.2 \pm 2.1$ MPa, strikes N1°W and dips 2°; 3) $\sigma_3 = 3.4 \pm 2.1$ MPa, strikes N91°W and dips 13°. Overcoring method was used to measure the in-situ stresses, and the location of the measuring point is marked in Fig. 1(a). The principal ground stress has a dip angle less than 90°, and its magnitude is much smaller than that calculated by the overburden weight due to the highly uneven ground surface as shown in Fig. 1(b). The orientation of the principal ground stress is almost vertical to the cavern axis, which permits the modelling of cavern in 2-D without generating large moments on the plane of the model. The total performance of the cavern was assessed by 3-D simulation using code FLAC^{3D}. To deepen the understanding of the deformation behavior on typical cross-sections and the influence of discontinuities on local deformations, 2-D simulations on cross-sections A and B of the cavern (*see* Fig. 1(a)) were carried out by using DEM. The boundary conditions of the 2-D model are shown in Fig. 1(b). The upper and left boundaries of the model were set to stress boundary conditions with a coefficient of lateral pressure $k_0 = 0.6$. Roller boundaries were applied to the right and bottom sides to uphold the model.

Properties of Rock Masses and Discontinuities

In some former studies, especially some continuum-based analyses, the properties of rock masses and discontinuities obtained from experiments are generally experienced modifications to satisfy the requirements of numerical program or to prevent ill results, which could easily bring confusion to other engineers who are not familiar with the modifications. To establish a common assistant method to the construction of underground structure, in this study, the properties of rock masses and discontinuities of the cavern adopted in the numerical simulations used the values directly obtained from the in-situ and laboratory experiments without modifications.

The mechanical properties of the rock masses and discontinuities in the construction site are shown in Tables 1 and 2. The properties of rock masses were obtained from in-situ compression tests. A high performance direct shear test apparatus, which supports the shear tests under both Constant Normal Load (CNL) and Constant Normal Stiffness (CNS) boundary conditions, was adopted to evaluate the mechanical properties of the discontinuities in the field (Jiang et al., 2001, 2004, 2006). The CNS boundary condition accommodates the change in normal stress caused by the dilation of rock fractures during a shear process, and therefore provides more realistic representation for the rock fractures in deep underground. Plaster-based materials were used to copy the

Table 1. Mechanical properties of rock mass

Item	Unit	Intact part	Damage zone
Unit volume weight (γ)	kN/m^3	27.1	27.1
Modulus of elasticity (E)	MPa	20000	7200
Poisson's ratio (ν)	—	0.23	0.23
Cohesion force (c)	MPa	1.6	0.26
Tensile strength (σ_t)	MPa	0.22	0.04
Basic friction angle (ϕ)	deg.	60	60

Table 2. Mechanical properties of rock joints

Item	Unit	Value
Shear stiffness (K_s)	MPa/m	5.62×10^3
Normal stiffness (K_n)	MPa/m	1.17×10^4
Cohesion force (c_j)	MPa	0
Friction angle (ϕ_j)	deg.	20
Tension strength (σ_j)	MPa	0

surfaces of three typical rock fractures and generated three artificial rock modules. A number of artificial rock specimens were then manufactured based on these modules, by using which, more than 50 cases of shear tests were carried out under various normal stress and normal stiffness conditions (Jiang et sl., 2001, 2004). The normal stiffness k_n applied to the rock specimens in the shear tests was decided by expanding the infinite cylinder theory as described in (Jiang et al., 2001). The normal loading tests have been carried out on the rock specimens with and without fracture plain (with same dimension) to acquire the total normal displacement u_{total} and intact normal displacement u_{intact}, respectively. Then, the normal behavior of the fracture can be derived from $u_{fracture} = u_{total} - u_{intact}$, and the normal stiffness of rock fracture can be obtained from the normal displacement-normal stress curves. In a shear test, the slope of the shear stress-shear displacement curve from 0 to the peak shear stress represents the shear stiffness k_s of the rock fracture. The value of shear stiffness used in numerical simulation adopted the mean value of these slopes in the shear tests. The friction angle of rock fractures was obtained from the shear stress-normal stress curves by connecting the peak shear stresses at different normal stresses. Given that the discontinuities in this site are slightly weathered and the number of faults in cross-sections A and B is much smaller than the joints, the properties of faults and joints have been assumed to be coincident, to simplify the modelling of discontinuities. Intact rock in the model is considered as an elastic-perfectly plastic material that follows Mohr-Coulomb failure criterion. Slip failure of the rock joint is also governed by the Mohr-Coulomb criterion. The boundaries of the model are subjected to the stresses from the surrounding rock masses. Before excavation, equilibrium under the gravity of rock mass was achieved to consolidate the blocks in the model.

Modelling of Discontinuities

In general, the geometrical distribution characteriza-

tion of discontinuities is a fundamental query to complete a reliable discontinuous rock mass model. To satisfy the requirements of the prior design of the underground cavern, site surveys were carefully planned to characterize the geometrical and geological properties of discontinuities. An investigation tunnel was firstly excavated above the main cavern before excavation. Depending on this tunnel, a boring survey system was established to collect the relevant in-situ geological information. Four geometrical characteristics: 1) orientation, 2) numbers, 3) trace length, and 4) spacing, were determined for each joint set. The distributions of discontinuities in the construction site and in cross-sections A and B are illustrated in Figs. 2(a) and (b), respectively. Besides the discontinuities identified in prior surveys, in cross-section A, a set of rock joints was identified during the arch excavation. The joints distributed near the two sidewalls were identified according to the survey data of sidewall by using borehole camera during the bench excavation. A number of rock joints have also been found during excavation in cross-section B, although the number of discontinuities in cross-section B is fewer comparing to that of cross-section A. Since the newly found (sometimes newly generated) rock joints during excavation could significantly influence the performance of the cavern, the model of discontinuities needs to be updated during the excavation to improve the prediction accuracy, which will be discussed in **COMPARISON OF SITE MEASUREMENT DATA WITH NUMERICAL RESULTS** in detail. In UDEC program, each joint as demonstrated in Fig. 2 can be easily reproduced in the model by deciding the starting point, length and dip angle. The rock joint set can be easily modelled by inputting the dip angle, trace length, gap and spacing values. It should be noted that the non-persistent joints in UDEC model are deleted when the model execution begins. To overcome this problem, several fictitious joints connecting the heads of non-persistent joints to the boundary of model were generated. After several attempts, the orientations and mechanical properties of these fictitious joints were carefully chosen to minimize their effects on the total performance of the model.

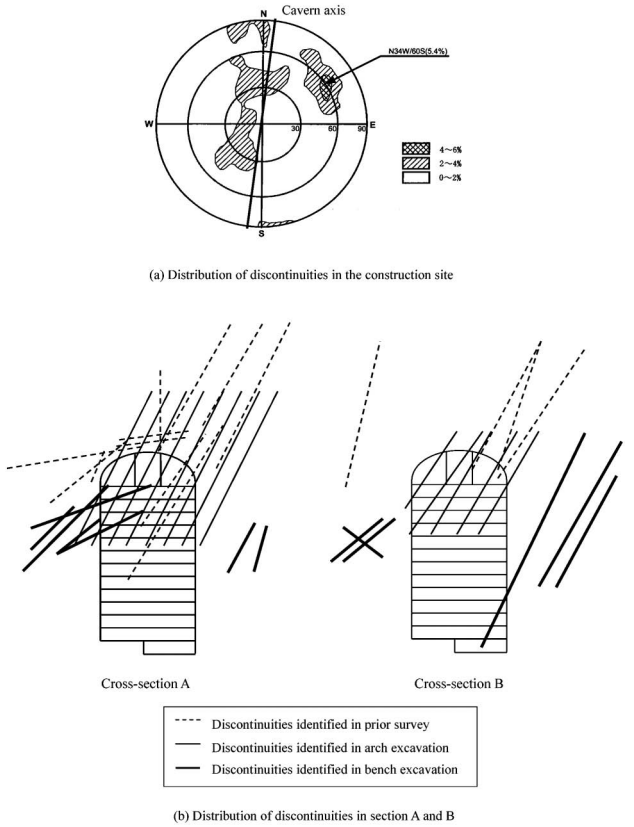

Fig. 2. The distribution of discontinuities in the construction site and identified in different stages of construction in cross-sections A and B

Excavation Process and Reinforcement Pattern

The procedure of bench-cut excavation and the design of reinforcement system used in this project are illustrated in Fig. 3. Rock bolts and prestressed anchors were

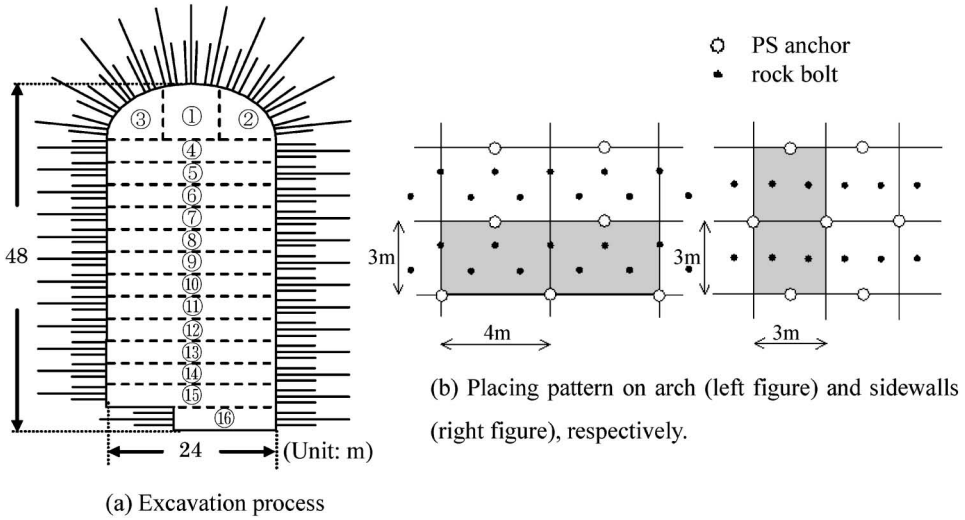

Fig. 3. Illustration of the Bench-cut excavation process and placing parttern of PS anchors and rock bolts on arch and sidewalls

used as reinforcements with a placing pattern as shown in Fig. 3(b). Rock bolts were installed in a pattern of 2 m × 2 m grid over the entire arch and a 3 m × 2 m grid on the two sidewalls.

The excavating process of the cavern is illustrated in Fig. 3(a). A pilot hole was drilled at the center of the arch at the first step. Then the left and right parts of arch were excavated in the steps 2 and 3. After that, bench excavation was carried out orderly from step 4 to step 16, of which, the excavated height in each step is 3 m. Reinforcement after the excavation in each step was conducted with an order as follows: (a) placing shotcrete, (b) embedding rock bolt, and (c) embedding PS anchor. The shotcrete was modelled as a structural element with a thickness of 0.32 m and the rock bolt and PS anchor were both treated as cable elements with different properties. The mechanical properties of rock bolt are: modulus of elasticity $E = 2.058\text{e}5$ MPa, cohesion $c = 0.1742$ MPa, tension $\sigma_t = 0.1765$ MPa. The mechanical properties of anchor are: modulus of elasticity $E = 1.862\text{e}5$ MPa, cohesion $c = 0.1742$ MPa, tensile strength $P = 0.46$ MN.

Influence of Damage Zone Caused by Blast

The damage zones that generated in the vicinity of cavern during blast have dramatic influence on the stability of the cavern due to their degraded strengths. According to the seismic exploration results as shown in Fig. 4, the regions of the surrounding rock masses with a thickness of around 2 m from the wall of cavern lost 60% of seismic velocity in comparison with the intact rock mass.

The following equation is proposed in (JSMS, 2002), relating the deformation coefficient (E) to the seismic velocity (V_p) as:

$$V_p = \sqrt{\frac{E}{\rho}\left(1 + \frac{2\nu^2}{1-\nu-2\nu^2}\right)} \quad (1)$$

where ρ is the unit weight of rock mass and ν is the Poisson's ratio. This equation provides an empirical relationship between seismic velocity and static modules. Using this equation, the modulus of elasticity E of the damaged rock masses surrounding the cavern is assessed as 36% of that of the undamaged rock masses. In the numerical model, the rock masses within the distance 2 m to the wall of cavern have been treated as blast damage zone with decreased mechanical properties as shown in Table 1.

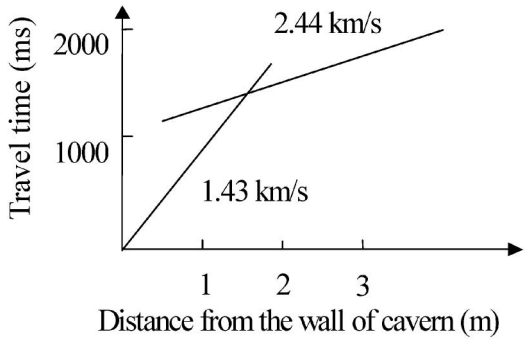

Fig. 4. Relationship of the seismic velocity with the distance from the wall of cavern

Displacement Monitoring

The information management of a construction project requires the in time information collection of the in-situ behavior during the construction process. To monitor the deformation behavior of the cavern in this project, a number of measurement instruments were placed in the investigation tunnels and drifts at various locations around the cavern. A layout of measuring lines in one cross-section is shown in Fig. 5. An investigation tunnel beyond the cavern starts 3 measuring lines (boring holes) to monitor the displacements on arch. 6 measuring

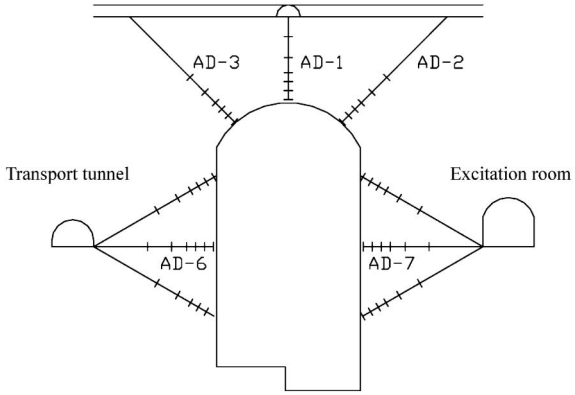

Fig. 5. A typical layout of the measuring lines (section A). Among them, numerical results of 5 lines (marked in the figure) were chosen to compare with the measurement results

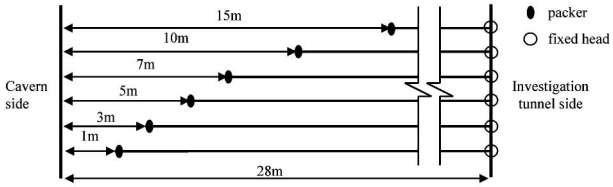

(a) The arrangement of displacement meters in one measuring line

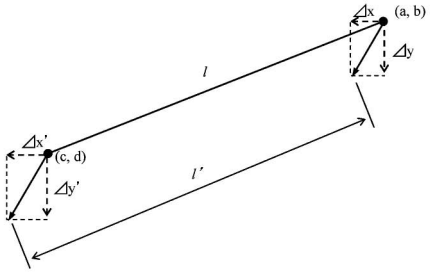

where $l = \sqrt{(a-c)^2 + (b-d)^2}$

$$l' = \sqrt{\{(a+\Delta x)-(c+\Delta x')\}^2 + \{(b+\Delta y)-(d+\Delta y')\}^2}$$

$$\Delta l = l' - l$$

(b) Calculation method of relative displacement Δl of each measuring line applied in analytical results.

Fig. 6. Sketch view of the arrangement of displacement meters in each measuring line and the disposal of simulation results to facilitate the comparison with the measurement results

lines connecting the transport tunnel and excitation room at the two sides of the powerhouse with the two sidewalls of cavern monitor the displacements on sidewalls. In each measuring line, 6 displacement meters with differing lengths were placed, of which the heads at the investigation tunnel side are all fixed together as shown in Fig. 6(a). Therefore, each displacement meter actually measures the relative displacement between the fixed head in the investigation tunnel and the packer of the meter in the boring hole. The displacement histories of these measuring lines have been recorded during the numerical simulations and have been transformed to the relative displacement (*see* Fig. 6(b)) to directly compare with the field measurements.

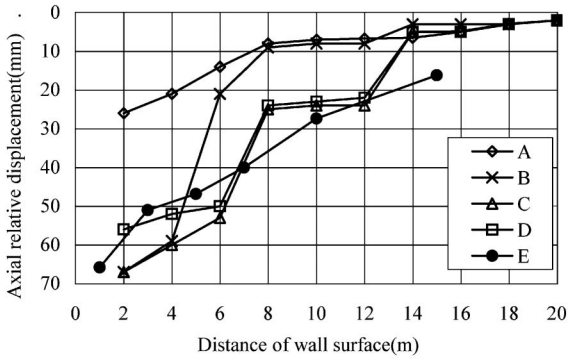

A : basic model based on prior survey
B : model added the discontinuities identified in arch excavation
C : model added the discontinuities identified in bench excavation
D : model added peripheral investigation tunnels
E : site measurement values

Fig. 7. Comparison of the simulation results of the models constituted at different construction stages with the measurement results

COMPARISON OF SITE MEASUREMENT DATA WITH NUMERICAL RESULTS

The modelling procedure used in this study can be summarized as: (1) carefully planning the prior survey to acquire effective geological data; (2) carrying out adequate in-situ and laboratory experiments based on reliable apparatus by effective methods to obtain the properties of rock masses and discontinuities; (3) inputting these geological engineering data into DEM program to build the basic numerical model; (4) updating the model of discontinuities during the excavation process to improve the representation of geometrical distributions of discontinuities and the accuracy of prediction and (5) advising the construction using the predicted results such as the reinforcement on key blocks. By following such a procedure, the simulation results were compared with measurement results as shown below.

Influences of the Input Discontinuity Distributions on the Behavior of Cavern

A well-planned prior survey is required to acquire sufficient geological data of the construction site so as to conduct a reliable design. As long as the rock masses are not excavated, a lot of geological features such as the presence of faults and joints are hidden in the field and are not easy to be identified by the prior survey. These newly found geological features, especially newly identified discontinuities during excavation need to be reflected in the revised numerical model to improve the accuracy of prediction. To elucidate the importance of considering adequate joint distributions in the numerical model, the numerical results of measuring line AD-6 (the center of left sidewall of cross-section A, as shown in Fig. 5) by inputting different joint distributions identified at the stages of prior survey, arch excavation and bench excavations, respectively (*see* Fig. 2), are compared and illustrated in Fig. 7. Herein, displacements were measured when the corresponding excavation step was finished. The models were re-executed from the start of excavation after each update of joint distribution.

Comparison of the results of cases A and B shows that case B provides much closer predictions to the site measurement E, which indicates that the joint set located at the arch remarkably affect the deformation behavior of the sidewall. Case C improves the accuracy of prediction by adding the joints near the sidewall. In case D, the transport tunnel and the excitation room at the two sides of the main cavern have been added; this slightly decreased the displacement at the sidewall of cavern due to the stress release produced by the excavations of the transport tunnel and the excitation room. The differences of cases A, B, C and D reveal the importance of the accurate configuration of discontinuities in a numerical model when analyzing an underground cavern. A thorough prior survey of geological information, especially the distribution of discontinuities needs to be designed and executed before construction to aid the support design. During the construction, the newly identified geological features (i.e., faults, joints) need to be incorporated into the numerical model, timely to provide better predictions of the behavior of underground structure.

Deformation Behavior Prediction by Numerical Simulation

The cross-sections A and B shown in Fig. 1 have been chosen to generate the 2-D numerical models. As described in section *Modelling of Discontinuities*, in cross-section A, a set of rock joints are located at the arch and a few joints are distributed near the sidewalls. Cross-section B has fewer joints at the arch and a few joints have been identified near the two sidewalls. By taking into account the last version of joint distributions of cross-sections A and B illustrated in Fig. 2, the numerical models are able to cover the most significant geological features of the construction site.

The distribution of plastic zones after the excavation steps 3, 8 and 16 of the cross-sections A and B are illustrated in Fig. 8. It should be noted that fictitious joints have been deleted to make a clear demonstration of the correlation of plastic zones with the location of pre-existing rock joints. The plastic zones include shear and tensile failures. Herein, only their location and total area are

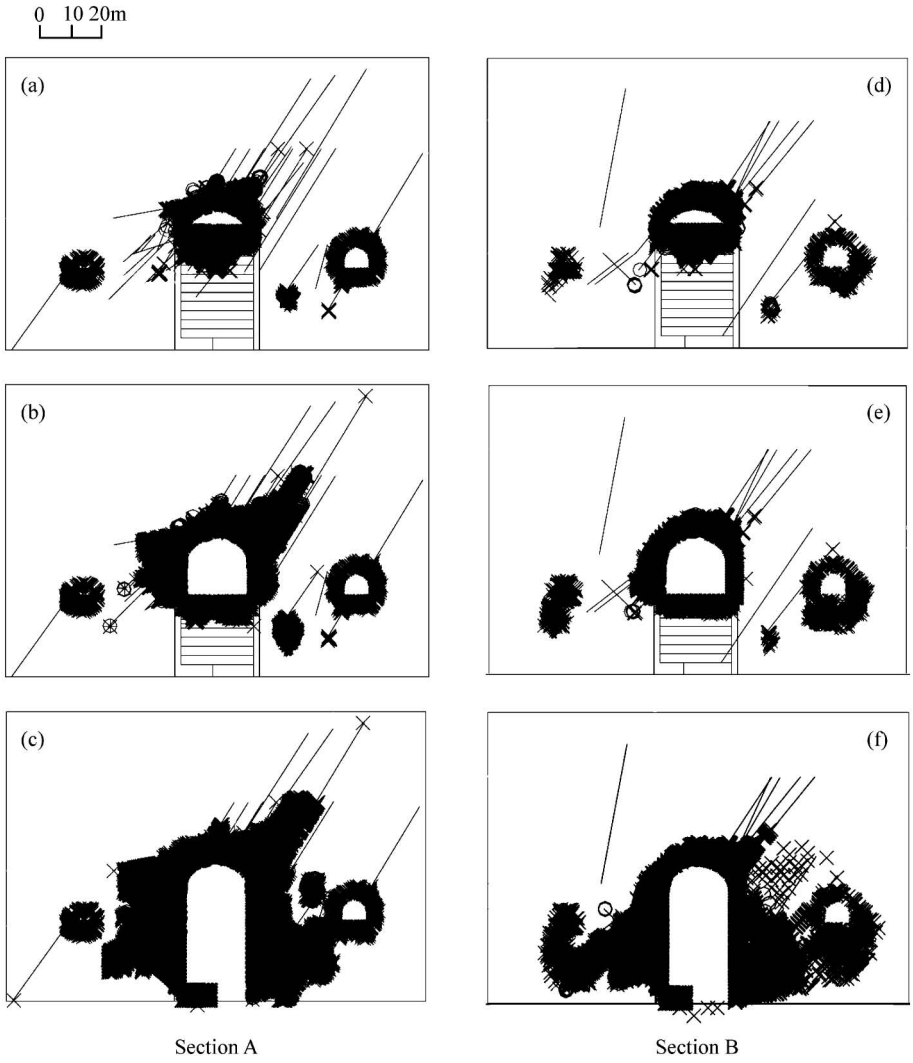

Fig. 8. Distribution of plastic zones after excavation steps 3, 8 and 16 of sections A ((a), (b) and (c)) and B ((d), (e) and (f)). The fictitious joints have been deleted to make a clear demonstration of the plastic zones and real rock joints

demonstrated. The excavation of arch released the stresses distributed on the roof and the bench floor, generating an elliptical plastic zone. The influence of the presence of rock joints on the plastic zone is not obvious until step 3, after that, the plastic zones start to propagate from the area close to the wall of cavern towards the highly jointed areas along the orientation of rock joints as shown in Figs. 8(b), (c), (e) and (f). The most significant progress of plastic zones occurs at the right upper corner of cross-section A, where a set of rock joints exists. As the bench excavation progresses, the plastic zones extend to the lower part of the rock masses encompassing the cavern, connecting with the plastic zones around the transport tunnel and the excitation room, forming a large plastic area. Cross-section A produces larger plastic zones than cross-section B especially around the arch (Figs. 8(c) and (f)), causing larger deformation in the vicinity of cavern as shown in Fig. 9. Since the rock blocks are permitted to rotate, slip and separate from each other in the DEM, high attention on the movements of the key blocks near or on the wall of cavern needs to be paid. In the present study, the presence of rock joint set on the arch divides the rock mass to small blocks, which is highly unfavorable to the stability of the arch. The falling of rock blocks was restrained by conservatively placed rock bolts and anchors; however, the key blocks on the left center of arch still exhibited large deformation in comparison with the right part of arch (*see* Fig. 9). In this case, the convergence of the displacements of these key blocks has been confirmed in the field and in the numerical model and therefore further reinforcements were not conducted. In some other cases, large deformations of such key blocks may develop to the principal risk to the stability of cavern and therefore requires special treatments. Large deformations also happen on the top of the left sidewall of cross-section A due to the presence of rock joints in the vicinity, exhibiting a toppling failure characteristic. Comparing with cross-section A, the displacements on the sidewalls of cross-section B with few joints are generally uniformly distributed along the wall surfaces, noting that there are more discontinuities encountering the sidewalls in cross-section A than cross-section B, which produce

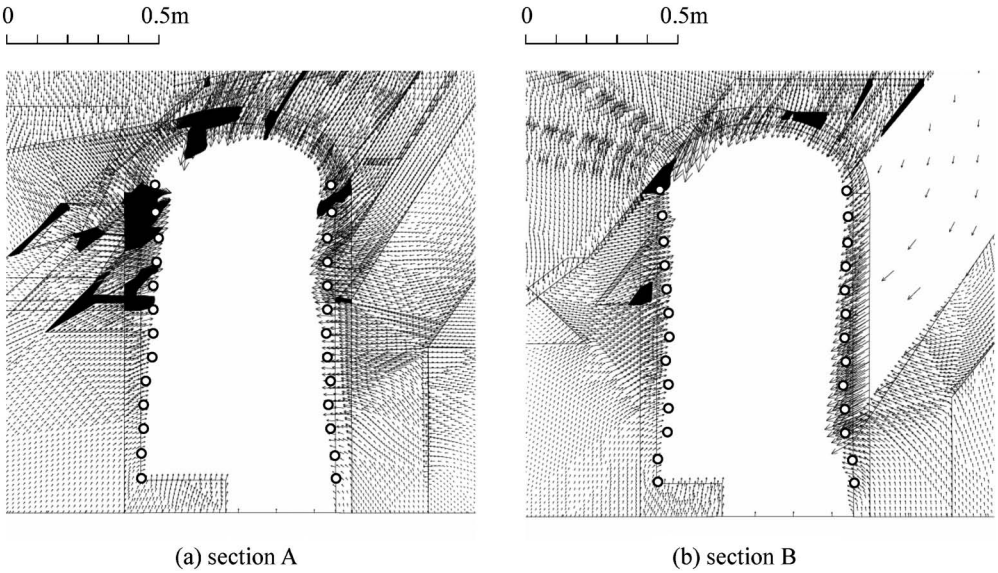

Fig. 9. Displacement vectors of sections A and B after the excavation of cavern. The black parts in the figure are the blocks with area less than 3.0 m^2, which, in the scale of this study, easily produce large deformation when encountering the walls of cavern. The distances between the hollow points and the sidewalls present the measured displacements on the wall of cavern

more rock blocks, one face of which is the component of the sidewall surface. The stresses on these faces are released after excavation, which are benefit to produce large deformation. The simulation results in Fig. 9 are slightly larger than the measured displacements on the wall of cavern, indicating that 2-D simulation may overestimate the deformation on the wall especially the deformation of key blocks.

Comparisons of Displacements Obtained by Site Measurement and Numerical Simulation

The comparisons of the displacements of cross-sections A and B from site measurements and numerical simulations in detail are illustrated in Fig. 10. The deviations of simulation results from the measured results were calculated through the equation of $D = (\text{simulation} - \text{measurement})/\text{measurement} \times 100\%$. The displacements of the arch in cross-section A happened in the construction site are around 30 mm at 1 m away from the roof of cavern and decrease gradually to around 10 mm at 15 m away from the roof as shown in Figs. 10(a), (b) and (c). The simulation results 2 m away from the cavern wall underestimate the displacement at AD-1 by around 35%. Better agreements can be found at other measuring lines especially at AD-2. Comparing the four typical measurement points at excavation steps 3, 8, 10 and 16 in Figs. 10(a), (b) and (c), it shows that the displacements at arch barely increase as the bench excavation progresses, indicating that when the excavation and reinforcement of arch have been completed, the subsequent excavation steps take little effect on the deformation on arch. Comparing with the arch, the deformations on the sidewalls increase continuously during all of the excavation steps especially in the last few steps as shown in Figs. 10(d) and (e). The most remarkable displacements occur at measuring line AD-6 due to the presence of discontinuities near the left sidewall (*see* Fig. 2) and the unfavorable orientation of initial ground stresses which will be discussed in the next chapter.

The discontinuities can encounter the sidewalls of an underground cavern with various angles. On AD-6 side, the rock joints dip away from the left sidewall and the blocks divided by these rock joints trend to fall into the cavern. On the contrary, the rock joints on AD-7 side, where the blocks trend to slip into the cavern, dip towards the right sidewall. In the prior design stage of this project, the AD-7 side (dipping towards pattern) was considered to be more dangerous to cause large deformation, since the blocks seem to be easier to slip into the cavern. However, both the site measurements and numerical simulation give the opposite results. In deep underground, due to the high stress environment, the slipping of rock blocks is significantly limited by the constraints from the surrounding rock blocks. The toppling failure happening in the ''dipping away pattern'' like AD-6 may have a better chance to cause large deformation. Based on the measurement data, further reinforcements have been conducted in the construction site on AD-6 side in terms of increasing the length of PS anchors referring to the simulation results. A study on the simple models of dipping towards pattern and dipping away pattern has also been carried out in (Jiang et al., 2006), indicating that in the jointed rock masses, the dipping away pattern produces lager displacement than the dipping towards pattern when the dip angle of joints is around 60°.

The simulation results of cross-section B are illustrated in Figs. 10(f)–(j). Because the length and number of the rock joints near the arch of cross-section B are smaller than that of cross-section A, on the same stress boundary condition the displacements of cross-section B at the arch are much smaller than the cross-section A (*see* Figs. 10(f), (g) and (h)). Due to the same reason, the displace-

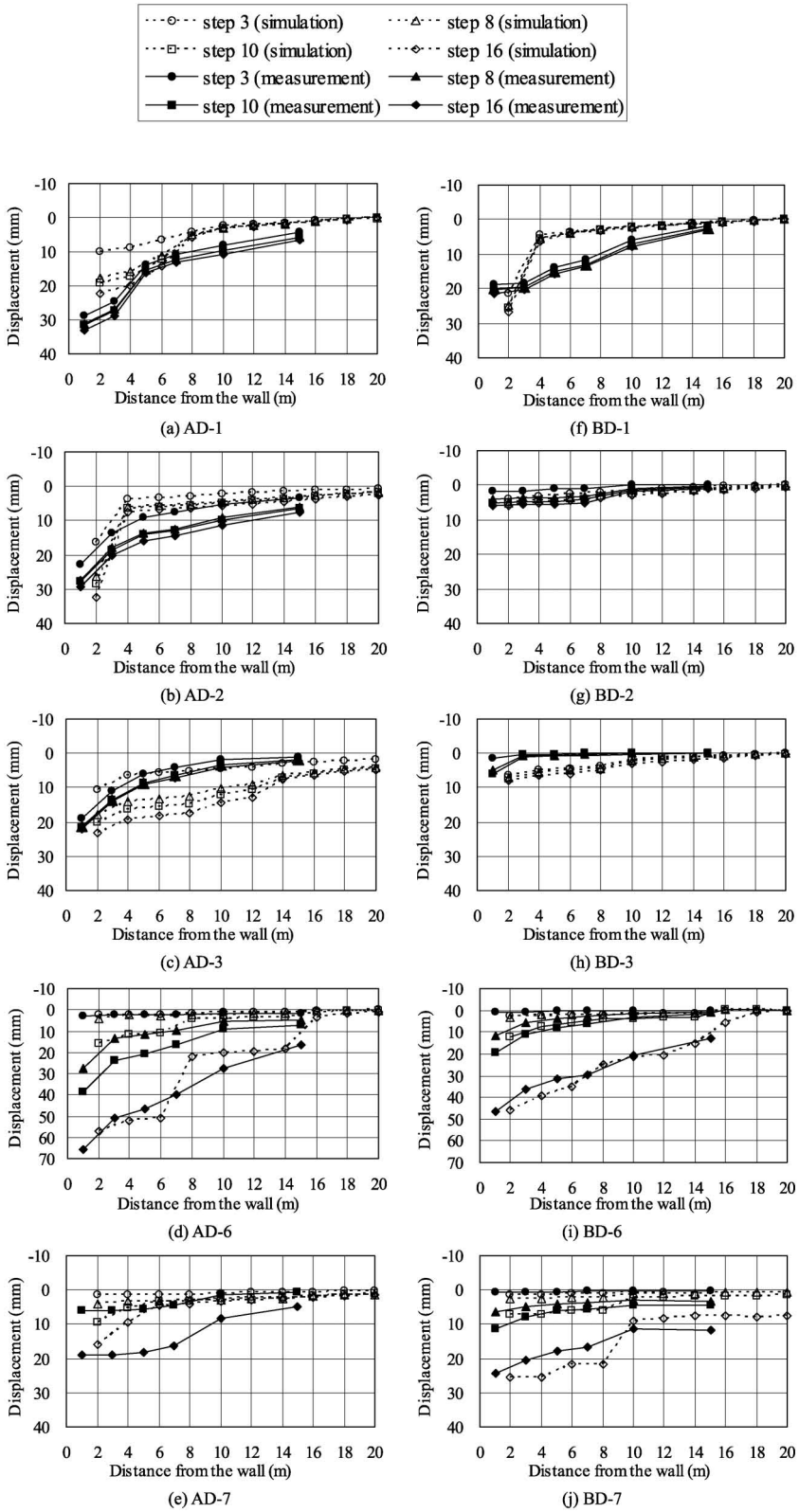

Fig. 10. Comparisons of the displacements obtained from site measurements and numerical simulations in four excavation steps of cross-setions A and B. Herein the displacements are the relative displacements measured by each measuring meters starting from the fixed heads located 28 m away from the walls of cavern as demonstrated in Fig. 6

ments at BD-6 are 1/3 smaller than AD-6 after all the excavation steps. A few discontinuities exist on the measuring line BD-7 (*see* Fig. 2), the normal and shear movements of which cause slightly larger displacements than that of AD-7. For cross-section B, the dipping away pattern (BD-6) also has larger displacement than the dipping towards pattern (BD-7) although the discontinuities on the two sides are almost equivalent in amount.

In both cross-sections A and B, the displacements on the sidewalls increase significantly with the progress of excavation especially in the last few steps. The convergence of displacements has been subsequently confirmed in both the site measurements and numerical simulation. The deviations of the results at the positions 4 m–10 m apart from the wall (around 40%) are much larger than that close to the wall. The maximum deviation occurs at BD-3, where the measured displacements are almost 0 and the simulation results are several millimeters, leading to large deviation values. For most of the other measuring points, the deviations are less than 20% at 2 m away from the wall of the cavern; therefore, generally speaking, the simulations provided good predictions to the displacements at the positions close to the wall of the cavern. In the positions several meters apart from the wall (e.g., 10 m), large discrepancies occur, mainly due to the following issues: 1) the rock masses are heterogeneous and their properties vary position by position; 2) the discontinuities can hardly be fully discovered and modelled in numerical simulation, especially the deformations of relatively small rock blocks located along measuring lines were not well represented (e.g., 4 m–10 m); 3) the application of mean mechanical properties to all the discontinuities compromised the representation of the behavior of discontinuities, since the properties of discontinuities can alter one by one; 4) the limitations of 2-D models in comparison to the real state of field.

INFLUENCES OF CROSS-SECTIONAL SHAPE AND ORIENTATION OF INITIAL GROUND STRESS

The cross-sectional shape of the cavern and the orientation of initial ground stresses are important factors influencing the performance of cavern. The cross-sectional shape of a cavern needs to be carefully chosen, synthetically considering the ground conditions, safety, function of cavern, cost etc. Warhead shape, egg shape and mushroom shape are typical cross-sectional shapes adopted in underground caverns. Since warhead shape

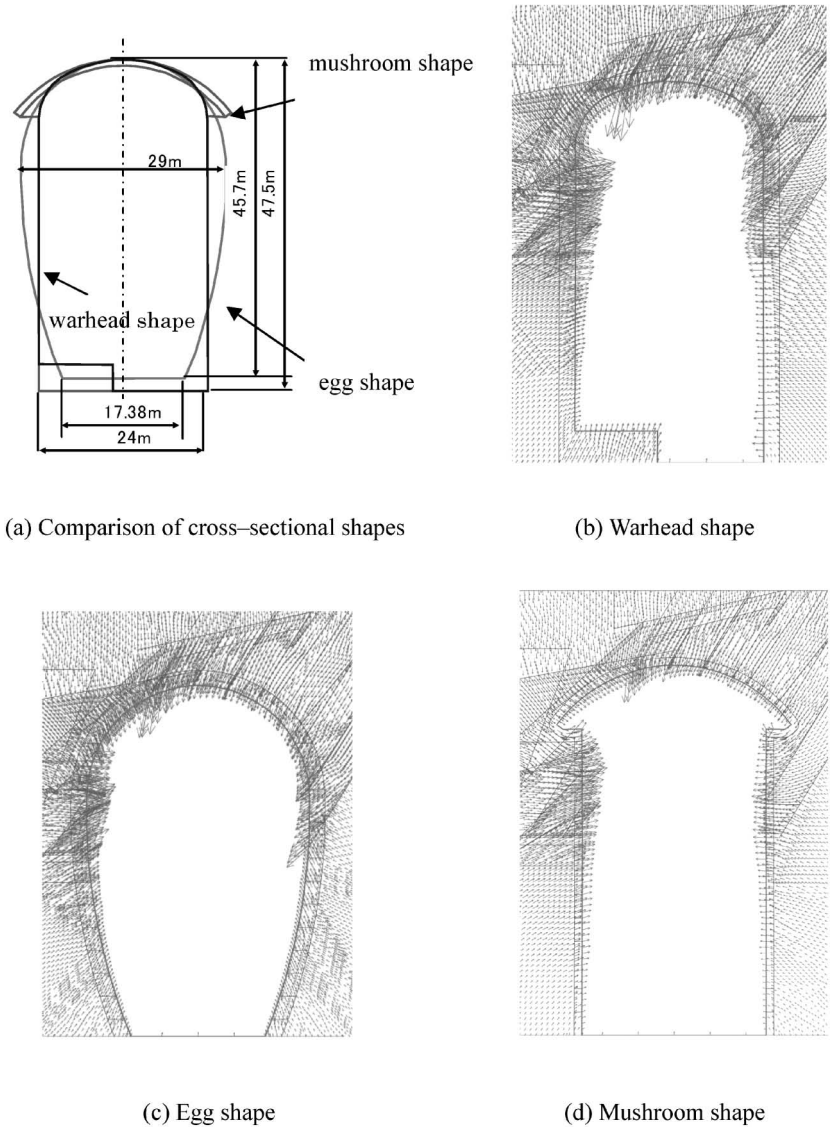

Fig. 11. Comparison of the displacement vectors around three types of cross-sections ($\theta = 0°$)

has been analyzed above, herein, numerical simulations on egg shape and mushroom shape are carried out based on the ground conditions of Omaru power plant (cross-section A) to assess the performance of cavern with different cross-sectional shapes at the same ground condition. The orientation of initial ground stresses impacts on the performance of cavern in terms of facilitating (unfavorable orientation) or restraining (favorable orientation) deformations of the rock masses surrounding a cavern. This impact is evaluated by changing the orientation of initial ground stress in the model of cross-section A as shown in Fig. 2.

The layout of three kinds of cross-sectional shapes is shown in Fig. 11(a). The cross-sectional area for warhead shape is 950 m^2, for egg shape is 1120 m^2 and for mushroom shape is 1120 m^2, noting that for mushroom shape, the thickness of lining concrete on arch is 1 m, which is thicker than other shapes (0.32 m) according to the thickness used in similar construction sites. The center top points of the arches of the three shapes are located at the same coordinate in numerical models and the heights and widths of egg and mushroom shapes were decided by considering the spaces required for installation of generators and constructability etc. referring to the data of Omaru power plant.

The comparison of the displacement vectors of the three kinds of cross-sectional shapes is shown in Figs. 11(b), (c) and (d). The warhead shape exhibits the largest displacement and the egg shape effectively inhibits the displacements especially on the sidewalls. For the egg shape, the arch integrates with sidewalls by smooth curves which improve the integrity of the arch and sidewalls, helping disperse stresses on the joint parts of arch and sidewalls. The mushroom shape remarkably inhibits the displacement of arch through its thick lining concrete on arch. The displacements on its sidewalls are smaller than the warhead shape, since its compressed arch shape and thick lining concrete have good effects in supporting the rock masses upon the arch while decreasing the pressures on sidewalls.

Initial ground stress is not always vertical to structure axes especially when an underground structure is located in a mountain area. To account for the influence of this factor, a series of orientations of initial ground stresses, $\theta = 0°, 20°, 35°, 50°, -20°, -35°, -50°$ with respect to vertical plane (positive for counter clock-wise) were examined on the models with different cross-sectional shapes based on the ground condition of cross-section A.

The simulation results of displacements along three measuring lines (AD-1, AD-6 and AD-7) are shown in Fig. 12, in which, Fig. (a) shows the results at measuring point 4 m away from the inner surface of cavern; Fig. (b)

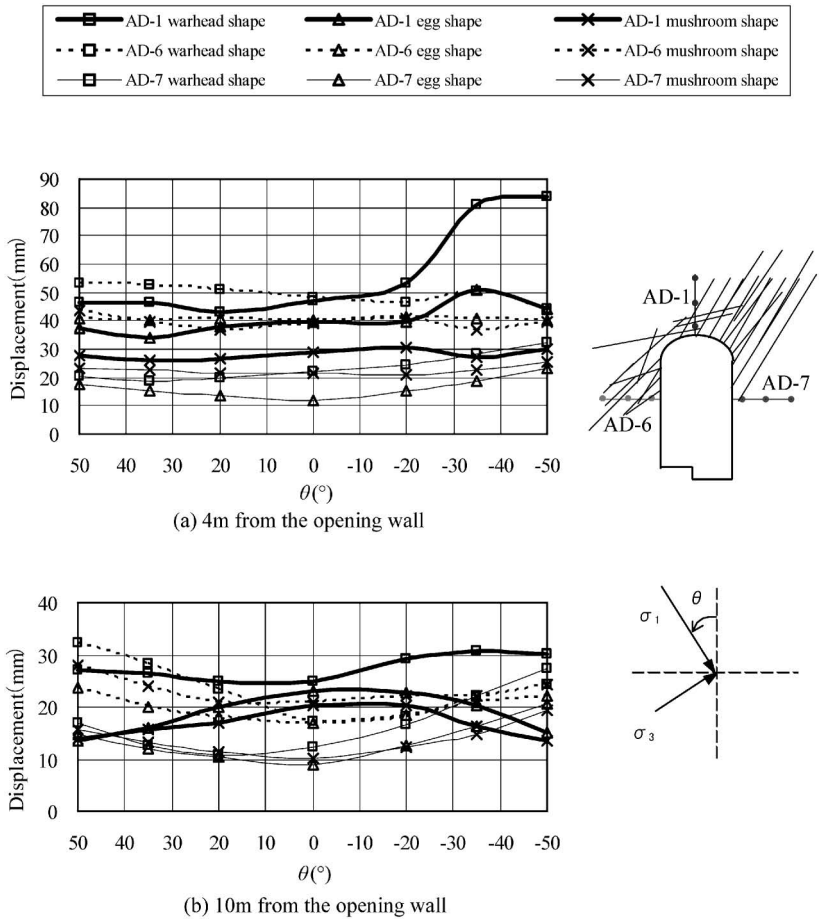

(a) 4m from the opening wall

(b) 10m from the opening wall

Fig. 12. Change of displacements due to the orientation of initial ground stress for three different cross-sectional shapes

shows the results at 10 m away from the inner surface of cavern. In Fig. 12(a), both warhead shape and egg shape exhibit an increase of displacement when $\theta = -35°$ at measuring line AD-1, and warhead shape has even higher value when $\theta = -50°$. The angles between $-35°$ and $-50°$ are coincident with the dipping angle of the pre-existing rock joints at the arch of cavern (*see* Fig. 2(b)), indicating that the orientations of initial ground stresses close to the pre-existing rock joints are unfavorable to the arch stability of cavern. This effect on mushroom shape is small due to its strong crown. The influences of the orientation of initial ground stress on measuring lines AD-6 and AD-7 are small comparing to measuring line AD-1. Generally, the displacements on sidewalls trend to decrease when the orientation of initial ground stress gets closer to vertical plane (90°).

As shown in Fig. 12(b), the influences of the orientation of initial ground stress become smaller when the distance apart from cavern wall increases. Similar to the results in Fig. 12(a), the displacements of measuring lines AD-6 and AD-7 increase as θ increases, indicating that large θ is unfavorable to the stability of sidewalls. For measuring line AD-1, three shapes have similar displacements when $\theta = 0°$, after that, egg shape and mushroom shape decrease and warhead shape increases as θ increases. The results of AD-1 in two figures show that egg shape and mushroom shape have more advantage in inhibiting the displacements on arch than warhead shape.

CONCLUSIONS

The reinforcement effect and stability of large-scale rock caverns in deep underground are often affected by discontinuity-related deformation. The presence of discontinuities in the vicinity of a cavern can significantly increase the area of plastic zones and the local deformation, especially when the joints encounter the wall of cavern. The DEM is capable of presenting the separation, rotation, slip and compression of discontinuities and therefore could be used to evaluate the local deformation behavior such as the movements of key blocks, which attract great concern in ensuring the stability of a cavern especially at arch in the jointed rock system. Souley et al. (1997) indicated that a simpler model (e.g., Mohr-Coulomb), with the correct parameters, matches the performance of more elaborate models (e.g., Cundall's C-Y model). Therefore choosing reliable mechanical properties is one of the key problems in modelling a cavern rather than attempting various constitutive laws. The main discontinuity distribution in a construction site can be captured by carefully planned boring survey system. Evaluation of the mechanical properties requires reliable in-situ and laboratory experiments.

In the present study, 2-D DEM was used for analyzing the stability of an underground powerhouse located in the jointed rock masses. The properties of rock masses were obtained through in-situ experiments and the mechanical properties of rock joints were estimated through direct shear tests using a high performance direct shear apparatus. The joint distribution in the numerical model was first determined using the data of prior geological survey, and the model was continuously updated when the new joints or faults were identified during arch and bench excavations. The model containing the version of joint distribution confirmed after the whole excavation provided the closest results to the site measurements at various positions in two typical cross-sections. The discontinuities at the upper part of a cavern (especially around arch) have remarkable influence on the deformation behavior of the whole cavern. The bench excavations affect the deformation on the arch little but continuously increase the deformation on sidewalls. The dipping away pattern of rock joints encountering the sidewall may produce lager displacement than the dipping towards pattern when the dip angle of joints is close to 60°. The egg shape and mushroom shape cross-sections were furthermore introduced into simulations based on the ground conditions of the original warhead shape model. The results revealed that orientations of initial ground stress close to the major pre-existing rock joints are unfavorable to the arch stability of cavern. Egg shape and mushroom shape have more advantage in inhibiting the displacements on arch than warhead shape.

The accuracy of simulation by using DEM significantly depends on the reliability of discontinuity distribution in a numerical model. In an underground cavern excavation field, however, the discontinuities usually cannot be fully discovered, which explains the story why the simulation results agree well with the measurements at some positions but differ at others. In this study, by following the modelling procedure based on the direct shear test-DEM approach, the numerical simulations have provided reasonably well predictions to the deformation behavior of the underground cavern as well as assessed the support effects of rock bolt and anchor. Integrating with the routine 3-D method, it could be used as an assistant design tool in underground constructions.

ACKNOWLEDGEMENTS

The authors wish to thank Mr. K. Nagaie, Mr. S. Morio and Mr. K. Goto for their assistance throughout this study. This study has been partially funded by Kyushu Electric Power Co., the Ministry of Education, Japan, Grant-in-Aid for Scientific Research (B), Research Project Number 11555131 and the National Natural Science Foundation of China (No. 50028403).

REFERENCES

1) Bhasin, R. K., Barton, N., Grimstad, E., Chryssanthankis, P. and Shende, F. P. (1996): Comparison of predicted and measured performance of a large cavern in the Himalayas, *Int. J. Rock Mech. Min. Sci.*, **33**, 607–626.
2) Bhasin, R. and Hoeg, K. (1998): Parametric study for a large cavern in jointed rock using a distinct element model (UDEC-BB). *Int. J. Rock Mech. Min. Sci.*, **35**, 17–29.
3) Cundall, P. A. (1993): A computer model for simulating progressive large scale movements in blocky rock system, *Proc. Symp Int.*

Soc. Rock Mech., Nancy, 1993, France, **1**.
4) Hao, Y. H. and Azzam, R. (2005): The plastic zones and displacements around underground openings in rock masses containing a fault, *Tunnelling Underground Space Technol.*, **20**, 49–61.
5) Itasca Consulting Group, Inc. (1998): UDEC-Universal Distinct Element Code, Version 3.0, User Manual, Minnesota, USA.
6) Jiang, Y., Tanabashi, Y. and Mizokami, T. (2001): Shear behavior of joints under constant normal stiffness conditions, *Proc. 2nd Asian Rock Mechanics Symposium* (ISRM2001-2nd ARMS), Beijing, 247–250.
7) Jiang, Y., Tanabashi, Y., Li, B. and Xiao, J. (2006): Influence of geometrical distribution of rock joints on deformation behavior of underground opening, *Tunnelling Underground Space Technol.*, **21**, 485–491.
8) Jiang, Y., Xiao, J., Tanabashi, Y. and Mizokami, T. (2004): Development of an automated servo-controlled direct shear apparatus applying a constant normal stiffness condition, *Int. J. Rock Mech. Min. Sci.*, **41**, 275–286.
9) Jiang, Y., Li, B. and Tanabashi, Y. (2006): Estimating the relation between surface roughness and mechanical properties of rock joints, *Int. J. Rock Mech. Min. Sci.*, **43**, 837–846.
10) Kulatilake, P. H. S. W., Ucpirti, H., Wang, S., Radberg, G. and Stephansson O. (1992): Use of the distinct element method to perform stress analysis in rock with non-persistent joints and to study the effect of joint geometry parameters on the strength and deformability of rock masses, *Rock Mech. Rock Eng.*, **25**, 253–274.
11) Schwer, L. E. and Lindberg, H. E. (1992): Application brief: a finite element slideline approach for calculating tunnel response in jointed rock, *Int. J. Num. Anal. Methods Geomech.*, **16**, 529–540.
12) Shen, B. and Barton, N. (1997): The disturbed zone around tunnels in jointed rock masses, *Int. J. Rock Mech. Min. Sci.*, **34**, 117–125.
13) Society of Materials Science, Japan (JSMS) (2002): *Rock Mechanics*, Gihodo, Tokyo.
14) Souley, M. and Homand, F. (1996): Stability of jointed rock masses evaluated by UDEC with an extended Saeb-Amadei constitutive law, *Int. J. Rock Mech. Min. Sci.*, **33**, 233–244.
15) Souley, M., Homand, F. and Thoraval, A. (1997): The effect of joint constitutive laws on the modelling of an underground excavation and comparison with in situ measurements, *Int. J. Rock Mech. Min. Sci.*, **34**, 97–115.
16) Suorineni, F. T., Tannant, D. D. and Kaiser, P. K. (1999): Determination of fault-related sloughage in open slopes, *Int. J. Rock Mech. Min. Sci.*, **36**, 891–906.
17) Zhao, J. and Chen, S. G. (1998): A study of UDEC modelling for blast wave propagation in jointed rock masses, *Int. J. Rock. Mech. Min. Sci.*, **35**, 93–99.